

## Electro-thermal Modeling of Lithium Ion Batteries

Gaoussou Hadia FOFANA\*, Youtong ZHANG

Low Emission Vehicle Research Lab, Beijing Institute of Technology

LABOThermique Appliquée, ENI-ABT BAMAKO-MALI BP 242

No. 5, Zhongguancun South Street, Haidian District, Beijing 100081, P. R. China

\*Corresponding author, e-mail: fofanamali@yahoo.fr

### Abstract

*In this paper, the electro-thermal model of Lithium-ion battery for electric vehicles and its related application were studied. The spatial variations of electrode parameter and the reaction heat generated inside battery must be considered when developing an electro-thermal model of Lithium-ion battery for electric vehicles, to ensure the applicability of the developed model under different operating conditions. The results showed that: with increasing state of charge, the spatial variations of net reaction current density, lithium ion concentration on the surface of active material particles, activation overpotential, equilibrium electrode potential and electrical potential of solid phase are reduced, but the spatial variation of electrical potential of electrolyte phase is enlarged.*

**Keywords:** *lithium-ion battery, electrochemical-thermal coupling model, porous electrode, charging and discharging, MATLAB*

**Copyright © 2014 Institute of Advanced Engineering and Science. All rights reserved.**

### 1. Introduction

According to the shape of automotive Lithium-ion battery (LIB), automotive LIB categories can be divided into square LIB and cylindrical LIB. Both types of batteries have similar internal structures, mainly including positive and negative current collector [1], anode and cathode electrodes and diaphragm, positive and negative current collector together with electrode can be referred to as pole piece. Positive and negative current collector generally consists of aluminum foil and copper foil respectively [2]. Positive and negative electrodes are mainly composed of active substances, the positive electrode active material usually uses cobalt acid lithium ( $\text{LiCoO}_2$ ), manganese acid lithium ( $\text{Li}_y\text{Mn}_2\text{O}_4$ ), or lithium iron phosphate ( $\text{LiFePO}_4$ ), the cathode active material generally uses graphite, acetylene carbon black, beads, petroleum coke, carbon fiber and polymer pyrolysis or pyrolysis carbon, diaphragm mainly including polyethylene, polypropylene and so on [3].

Electrochemical-thermal coupling model should be in a reasonable model, including some considering factors and assumptions of the premise, ensuring the applicability and rationality of the model [4]. In order to ensure the electro-thermal coupling model for predicting power characteristics and the temperature rise characteristics of automotive LIB pack, the electrode parameters spatial difference and reaction heat generated by the battery charge and discharge process must be considered in the process of modeling [5]. Therefore, this paper considered the spatial variations of net reaction current density, lithium ion concentration on the surface of active material particles, activation overpotential, equilibrium electrode potential and electrical potential of solid phase in establishing automotive LIB electrochemistry-thermal coupling model. Then, this article used the established electrochemical-thermal coupling model to simulate the space distribution of electrode parameters and internal battery heat generated rate under different working conditions.

### 2. Research Method

LIB Solid-solution phase interface electrochemical reaction process can be actually decomposed into forward and reverse reaction. Ensuring the electrode on the two phase interface forward/reverse reaction rate and activation energy barrier changing extent is the key to calculate net current. According to the principle of kinetic reaction, the exchange current

density  $i_0$  ( $A/cm^2$ ) on the two phase interface, namely the interface reaction is in dynamic equilibrium, the forward/reverse reaction rate can be calculated by the Equation (1) [6]:

$$i_0 = kF (c_e)^{a_a} (c_{s\max} - c_{se})^{a_a} (c_{se})^{a_c} \quad (1)$$

In which,  $k$  is the electrode reaction rate constant (cathode, anode);  $F$  is Faraday constant;  $c_e$  is lithium-ion concentration in the solution phase;  $c_{s\max}$  is maximum lithium ion concentration of solid phase (cathode, anode);  $c_{se}$  indicates the lithium ion concentration on the solid and liquid phase interface (the active material particles surface,  $mol/cm^3$ );  $a_a$  is the anodic electron transfer coefficient,  $0 < a_a < 1$ , under normal circumstances,  $a_a = 0.5$ ; while  $a_c$  is the cathode electron transfer coefficient,  $0 < a_c < 1$ , under normal circumstances,  $a_c = 0.5$ . According to the principle of kinetics reaction, the activation overpotential  $\eta$  characterizes the two phase interface activation energy barrier changing extent,

$$\eta = \varphi_s - \varphi_e - U \quad (2)$$

Where,  $\varphi_s$  is the solid phase voltage (V);  $\varphi_e$  is potential of the solution (V);  $U$  is balanced electrode potential (V);  $U$  is mainly determined by the temperature of the battery and the electrode stoichiometric ratio  $\theta = c_{se} / c_{s\max}$ , their specific relationship should be confirmed by fitting test data. About electrochemical-thermal coupling model, the relationship between positive and negative electrode  $U$  and  $\theta$  is described based on battery temperature known.

Anode:

$$U = 8.00229 + 2.1765 \times 10^{-5} \theta^{1.5} + 5.0647 \theta - 12.578 \theta^{0.5} - 8.6322 \times 10^{-4} \theta^{-1} - 0.46016 \times \exp[15 \times (0.06 - \theta)] - 0.55364 \times \exp[-2.4326 \times (\theta - 0.92)] \quad (3)$$

Cathode:

$$U = 85.681 \theta^6 - 357.7 \theta^5 + 613.89 \theta^4 - 555.65 \theta^3 + 281.06 \theta^2 - 76.648 \theta - 0.30987 \times \exp[5.657 \theta^{115}] + 13.1983 \quad (4)$$

$U$  changing along with the change of the battery temperature is usually described by temperature coefficient  $\partial U / \partial T$ ,  $\partial U / \partial T$  mainly depends on LIB  $\theta$ , usually setting  $\theta$  known to character temperature coefficient  $\partial U / \partial T$ ; the relationship between  $\theta$  and state of charge (SOC) shows in (5).

$$\theta = 0.01 \times SOC \times (\theta_1 - \theta_0) + \theta_0 \quad (5)$$

In which,  $\theta_1$  is a stoichiometric ratio in the battery full charge state (SOC=100%);  $\theta_0$  is a stoichiometric ratio after the battery emitting the rated capacity (SOC=0%); SOC is equal to the ratio of the remaining power and battery capacity,

$$SOC = \frac{Q_e}{Q} = 1 - \frac{Q_0}{Q} \quad (6)$$

In the formula,  $Q_e$  is the remaining power in the current time,  $Q$  is the whole power of battery,  $Q_0$  is discharge capacity, usually SOC is belong to [0.2, 0.8] [7].

Figure 1 shows the active material particles  $LiFePO_4$  and  $Li_xC_6$  of positive and negative electrodes happen with the reduction reaction, temperature coefficient  $\partial U / \partial T$  changes along with the change of electrode stoichiometric ratio  $\theta$  [8]. As shown in Figure 2, the same amount of lithium ion in different SOC, the entropy change extent is very different by finishing de-intercalation reaction and re-intercalation reaction.

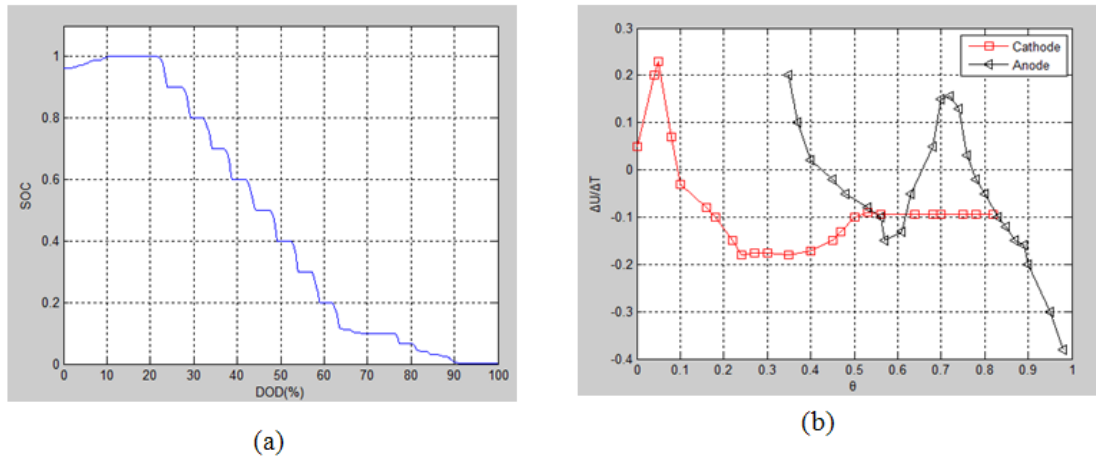


Figure 1. (a) SOC on variation of battery voltage versus depth of discharge (DOD); (b) variation of battery voltage versus battery temperature  $\partial U / \partial T$

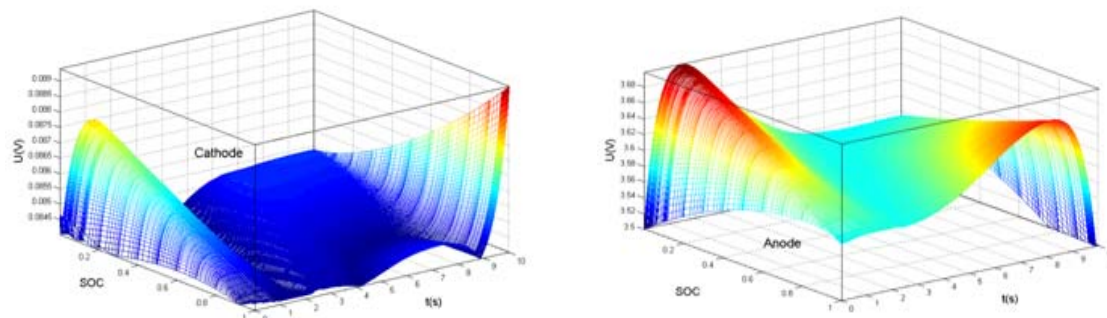


Figure 2. Positive and Negative Electrodes versus SOC

Figure 2 shows that with the decrease of the SOC, the open circuit voltage amplitude of the modeling objects decreases gradually. Accordingly, the smaller the SOC is, the smaller  $U$  changing along with  $\theta$  changing is. However, as for the two phase interface in unit volume of the electrode electrochemical reaction net current  $j$ ,  $j$  space distribution is different under different SOC during charging and discharging,  $j$  increases with the decrease of the SOC. At the same time, due to  $\theta$  dynamic change completely determined by  $j$ , hence,  $\theta$  increases with the decrease of the SOC. After respectively using (1) and (2) determine the exchange current density and activation potential, and then computing automotive LIB electrodes solid - solution phase interface reaction rate. By Butler-Volmer equation  $j$  is shown in (7) in detail:

$$j = s_e i_0 \left\{ \exp \left[ \frac{a_a n F}{RT_{bat}} \left( \eta - \frac{R_{SEI} j}{s_e} \right) \right] - \exp \left[ - \frac{a_c n F}{RT_{bat}} \left( \eta - \frac{R_{SEI} j}{s_e} \right) \right] \right\} \tag{7}$$

Where,  $j$  is the two phase interface in unit volume of the electrode electrochemical reaction net current,  $A/cm^3$ ;  $s_e$  is the average active area per unit volume;  $R=8.314J/(mol-K)$  is the general gas constant;  $T_{bat}$  is the battery temperature,  $K$ , and this paper used  $T_{bat} = 273+25K$ ;  $R_{SEI}$  is the active material particles surface passive film area resistance,  $\Omega \cdot cm^2$ .

According to ohm's law, the charge transfer flux produced by arbitrary cross-section conductors under the action of electrical driving force is equal to the product of the cross-section electric potential gradient and the conductivity. Combined with the law of conservation of electric charge, the relationship between the solid phase in porous electrode potential gradient and the net reaction current density is shown in (8):

$$\frac{\partial}{\partial x} \left( \sigma^{eff} \frac{\partial \varphi_s}{\partial x} \right) = j \quad (8)$$

The boundary conditions:

$$x=0, \sigma^{eff} \frac{\partial \varphi_s}{\partial x} = -\frac{I}{S_e}; x=\delta_n, \sigma^{eff} \frac{\partial \varphi_s}{\partial x} = 0; x=L-\delta_p, \sigma^{eff} \frac{\partial \varphi_s}{\partial x} = 0; x=L, \sigma^{eff} \frac{\partial \varphi_s}{\partial x} = \frac{I}{S_e}.$$

In which,  $I$  is the battery charging and discharging current,  $I>0$  indicates charging process,  $I<0$  shows discharging process,  $A$ ;  $S_e=1.0452 \times 10^4$  is the total activation area in the battery pole piece,  $cm^2$ ;  $\sigma^{eff}$  is the effective electrical conductivity of solid phase electronic,  $S/cm$ ;  $\sigma^{eff}$  can be calculated by (9):

$$\sigma^{eff} = \sigma \varepsilon_s^{pe} \quad (9)$$

In which,  $\sigma$  is solid phase electronic conductivity,  $S/cm$ ;  $\varepsilon_s$  is LIB positive and negative electrode active material volume fraction;  $pe=1.5$  is Bruggeman porosity factor. Hence, the cathode:  $\sigma^{eff} = 0.58$ ; the anode:  $\sigma^{eff} = 0.05$ .

Generally, due to porous electrode conductivity and diffusion coefficient variation are much smaller, so the electric potential gradient and concentration gradient are lithium ion (positive charge) driving force in the solution phase during the move. Hence, it cannot be able to directly use ohm's law to describe the net current density and solution phase electric potential gradient, and the equation modification [9] is shown below:

$$\frac{\partial}{\partial x} \left( \kappa^{eff} \frac{\partial \varphi_e}{\partial x} \right) + \frac{\partial}{\partial x} \left( \kappa_D^{eff} \frac{\partial \ln c_e}{\partial x} \right) + j = 0 \quad (10)$$

$$\text{The boundary conditions: } x=0, \frac{\partial \varphi_e}{\partial x} = 0; x=L, \frac{\partial \varphi_e}{\partial x} = 0.$$

In which,  $\kappa^{eff}$  is lithium-ion effective electrical conductivity of solution phase,  $S/cm$ ; the cathode:  $\kappa^{eff} = 3.9 \times 10^{-4}$ ; the diaphragm:  $\kappa^{eff} = 7.21 \times 10^{-4}$ ; the anode:  $\kappa^{eff} = 3.87 \times 10^{-4}$ ;  $\kappa_D^{eff}$  is effective diffusional conductivity coefficient of solution phase,  $A/cm$ . The  $\kappa^{eff}$  calculation formula is shown in (11).

$$\kappa^{eff} = \kappa \varepsilon_e^{pe} \quad (11)$$

Where,  $\varepsilon_e$  is the electrode porosity, that is to say  $\varepsilon_e$  is the volume fraction of the electrolyte;  $\kappa$  is lithium ion conductivity of solution phase,  $S/cm$ ,  $\kappa$  is completely determined by electrolyte composition. And according to the theory of strong solution,  $\kappa_D^{eff}$  can be calculated by the (12):

$$\kappa_D^{eff} = \frac{2RT_{bat} \kappa^{eff}}{F} \left( t_+^0 - 1 \right) \left( 1 + \frac{d \ln f_{\pm}}{d \ln c_e} \right) = \frac{2RT_{bat} \kappa^{eff}}{F} \left( t_+^0 - 1 \right) \quad (12)$$

In which,  $f_{\pm} = 1$  as the electrolyte activity coefficient [10][11];  $t_+^0 = 0.363$  for lithium ion transference number.

As for LIB charge and discharge procedure, part of the inner heat generated raises the temperature of the battery itself, another transmits to the battery surface sending out into the surrounding environment by conductive effect. So many physical and chemical parameters in LIB are associated with battery temperature values, including the electrode reaction rate

constant, the lithium ion diffusion coefficient, electronic electrical conductivity of the solid phase and solution phase lithium ion diffusion coefficient and electrical conductivity.

### 3. Results and Analysis

Reasonably calculating the spatial distribution of parameters in LIB electrodes and internal heat generated rate is to ensure that the model can be applied to predict automotive LIB pack power characteristics and the temperature rise. To illustrate the rationality of the electrochemical-thermal coupling model established in this paper, this section will simulate the spatial distribution of the net current density, lithium ion concentration, the activation over potential, electrode potential based on the model of the battery under 80% SOC [12].

Figure 3~Figure 6 presented LIB seconds pulse charging and discharging, the SOC changing effects the spatial distribution of the net reaction in positive and negative electrode current density  $j$ , active material lithium-ion concentration and the ratio of the maximum concentration  $c_{se}/c_{smax}$ , the activation over potential  $\eta$ , balanced electrode potential  $U$ . Figure 3 shows SOC=80% respectively, the temperature of the battery is 25°C, and charging and discharging currents are 5C.

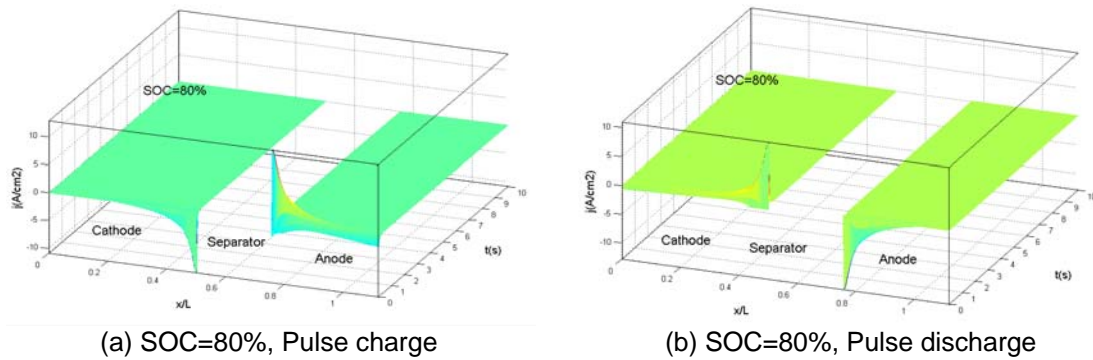


Figure 3. The Spatial Distribution of  $j$  in the Battery Pulse Charging and Discharging under 80% SOC ( $T_{bat}=25\text{ }^\circ\text{C}$ ,  $I=5C$ )

Figure 3 indicates under 80% SOC, in the initial moment of the LIB pulse charging and discharging, a peak of  $j$  is always produced near the electrode area of the diaphragm, but along with progress through the charging and discharging,  $j$  in the positive and negative electrodes gradually tend to be uniformly distributed along the  $x$  axes. However, with the battery charging and discharging progressing, heterogeneous reaction rate will gradually lead to the spatial variation increasing of  $c_{se}/c_{smax}$ .

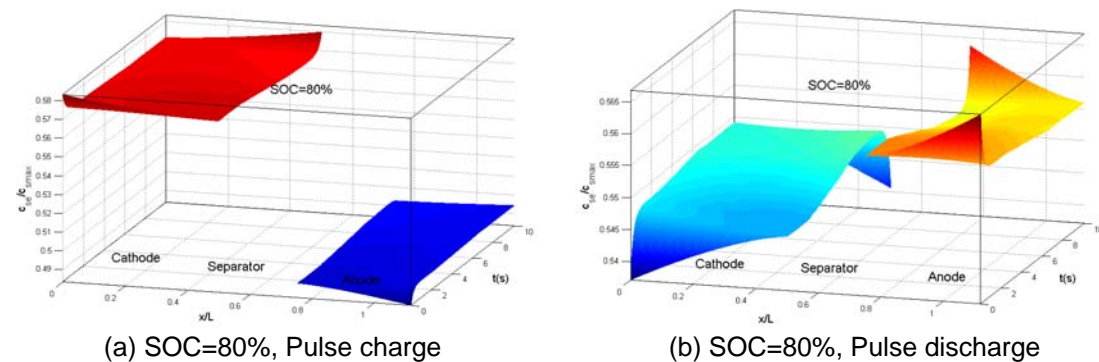


Figure 4. The spatial distribution of  $c_{se}/c_{smax}$  in the battery pulse charging and discharging under 80% SOC ( $T_{bat}=25\text{ }^\circ\text{C}$ ,  $I=5C$ )

As shown in Figure 4, the smaller the distance of the active material particles and the diaphragm is, the bigger lithium ion concentration increases or reduces. Relatively larger or smaller  $c_{se}/c_{smax}$  will result in lithium ions de-intercalation reaction and re-intercalation reaction more energy consumed.

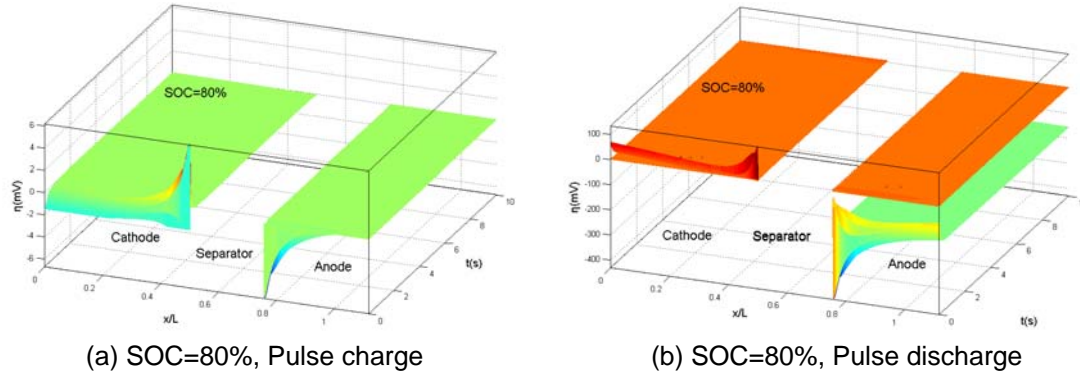


Figure 5. The Spatial Distribution of  $\eta$  in the Battery Pulse Charging and Discharging under 80% SOC ( $T_{bat}=25\text{ }^{\circ}\text{C}$ ,  $I=5C$ )

Figure 6 indicates the spatial distribution  $U$  of positive and negative electrode is similar to the  $c_{se}/c_{smax}$  spatial distribution in Figure 5 when Charging, the  $U$  value of the positive and negative electrodes gradually reduces along the  $x$  axis. In contrast,  $U$  increases along the  $x$  axis. Because the lithium ion concentration  $c_{smax}$  is smaller in the cathode active material particles than the anode's  $c_{smax}$ , that the same amount of lithium ions in the cathode progress de-intercalation reaction and re-intercalation reaction causes bigger change of  $c_{se}/c_{smax}$  than positive reaction. So generally speaking, a battery charging and discharging in the same current and different SOC, the space distribution variation of negative  $U$  is more apparent along the  $x$  axis than that of positive  $U$ .

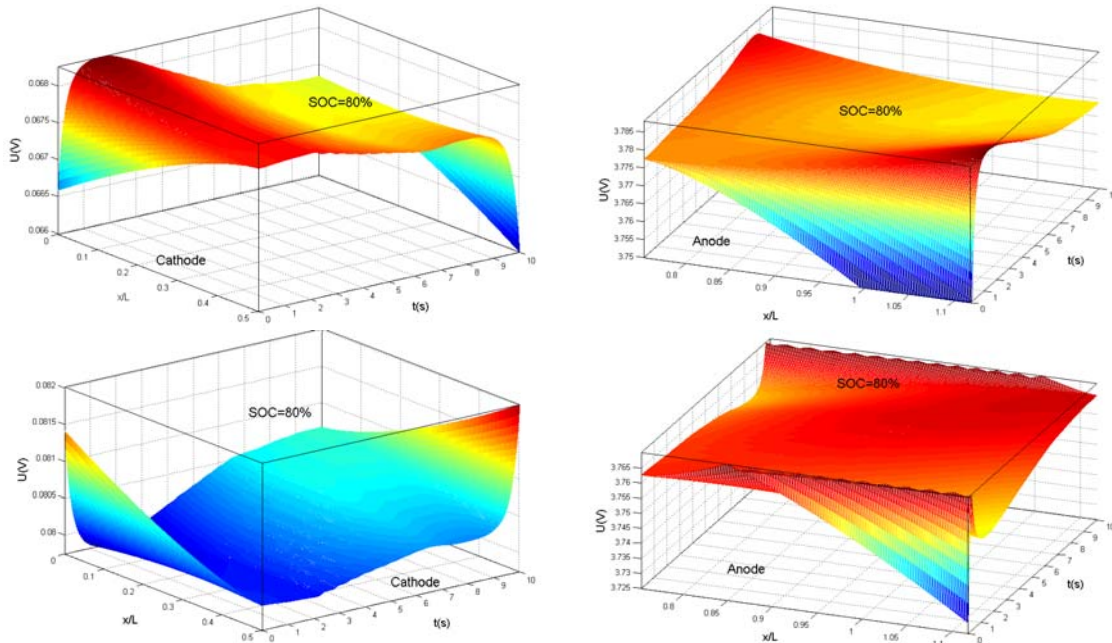


Figure 6. The Spatial Distribution of  $U$  in the Battery Pulse Charging and Discharging under 80% SOC ( $T_{bat}=25\text{ }^{\circ}\text{C}$ ,  $I=5C$ )

#### 4. Conclusion

Electrochemical-thermal coupling model should consider some more factors and assumptions to build a reasonable model to ensure the applicability and rationality of the model. An electro-thermal model of LIB for electric vehicles is developed based on the porous electrode theory with considering the spatial variations of electrode parameter and reaction heat, and the solution for the model to the effects of SOC, current rate and temperature on the spatial variations of electrode parameter and heat generation based on MATLAB language. The results indicate that: the spatial distribution  $\eta$  and dynamic change process is similar to  $j$ , SOC reduction will increase the spatial distribution difference of  $\eta$ . The spatial distribution  $U$  of positive and negative electrode is similar to the  $c_{se}/c_{smax}$  spatial distribution. When a battery charging and discharging in the same current and different SOC, the space distribution variation of negative  $U$  is more apparent along the x axis than that of positive  $U$ . Electrochemical-thermal coupling model to simulate the space distribution of electrode parameters and internal battery heat generated rate under different working conditions is reasonable and acceptable.

#### References

- [1] Dong Hyup Jeon, Seung Man Baek. Thermal modeling of cylindrical Lithium ion battery during discharge cycle. *Energy Conversion and Management*. 2011; 52(8-9): 2973-2981.
- [2] KM Abraham, SB Brummer, JP Gabano, *Editor*. Lithium Batteries. New York: Academic Press. 1983.
- [3] lezhou Wu, Lunan Liu, Qing Xiao, et al. Research on SOC estimation based on second-order RC model. *TELKOMNIKA Indonesian Journal of Electrical Engineering*. 2012; 10(7): 1667-1672.
- [4] WB Gu, CY Wang. *Thermal-electrochemical coupled modeling of a lithium-ion cell*. ECS Proceedings. 2000; 99-25(1): 748-762.
- [5] Lei Lin, Yuankai Liu, Wang Ping, Fang Hong. The Electric Vehicle Lithium Battery Monitoring System. *TELKOMNIKA Indonesian Journal of Electrical Engineering*. 2013; 11(4): 2247-2252.
- [6] Kandler A Smith, Christopher D Rahn, Chao-Yang Wang. Control oriented 1D electrochemical model of lithium ion battery. *Energy Conversion and Management*. 2007; 48: 2565-2578.
- [7] Wang Zhifu, peng lianyun, Sun Fengchun, etc. Charge and discharge characteristics of Li-ion batteries for EV. *Battery Biomonthly*. 2003; 33(3): 167-168.
- [8] Yonghuang Ye, Yixiang Shi, Ningsheng Cai, Jianjun Lee, Xiangming He. Electro-thermal modeling and experimental validation for lithium ion battery. *Journal of Power Sources*. 2012; 199: 227-238.
- [9] Marc Doyle, John Newman, Antoni S Gozdz, Caroline N Schmutz, Jean-Marie Tarascon. Comparison of modeling predictions with experimental data from plastic lithium ion cells. *Journal of the Electrochemical Society*. 1996; 143(6): 1890-1903.
- [10] Kandler A Smith, Chao-Yang Wang. Power and thermal characterization of a lithium-ion battery pack for hybrid-electric vehicles. *Journal of Power Sources*. 2006; 160(1): 662-673.
- [11] Weifeng Fang, Ou Jung Kwon, Chao-Yang Wang. Electrochemical-thermal modeling of automotive Li-ion batteries and experimental validation using a three-electrode cell. *International Journal of Energy Research*. 2010; 34(2): 107-115.
- [12] Ma Y, Teng H. Comparative Study of Thermal Characteristics of Lithium\_ion Batteries for Vehicle Applications. *SAE Technical Paper*. 2011; 2011-01-0668.